World Scientific
www.worldscientific.com

MECHANICAL FLEXIBILITY OF ZINC OXIDE THIN-FILM TRANSISTORS PREPARED BY TRANSFER PRINTING METHOD

K. T. EUN*, W. J. HWANG*, B. K. SHARMA†, J. H. AHN†,
Y. K. LEE* and S. H. CHOA*,‡

*Graduate School of NID Fusion Technology,
Seoul National University of Science and Technology,
172 Gongneung-2dong, Nowon-gu, Seoul, 139-743, Korea
†School of Advanced Materials Science and Engineering, Sungkyunkwan University,
Cheoncheon-dong 300, Jangan-gu, Suwon, 440-746, Korea
‡shchoa@seoultech.ac.kr

In the present study, we demonstrate the performance of Zinc oxide thin film transistors (ZnO TFTs) array subjected to the strain under high bending test and the reliability of TFTs was confirmed for the bending fatigue test of 2000 cycles. Initially, ZnO TFTs were fabricated on Si substrate and subsequently transferred on flexible PET substrate using transfer printing process. It was observed that when the bending radius reached ≥ 11 mm then cracks start to initiate first at SiO_2 bridges, acting as interconnecting layers among individual TFT. Whatever the strain is applied to the devices, it is almost equivalently adopted by the SiO_2 bridges, as they are relatively weak compared to rest of the part. The initial cracking of destructed SiO_2 bridge leads to the secondary cracks to the ITO electrodes upon further increment of bending radius. Numerical simulation suggested that the strain of SiO_2 layer reached to fracture level of 0.55% which was concentrated at the edge of SiO_2 bridge layer. It also suggests that the round shape of SiO_2 bridge can be more fruitful to compensate the stress concentration and to prevent failure of device.

Keywords: Transparent thin film transistor; zinc oxide; mechanical reliability; bending test.

1. Introduction

Fabrication of ZnO TFTs has attracted much attention for realizing the practical applications of flexible electronics, such as organic light emitting diode (OLED) display, radio frequency identification tag and smart card. The high mobility and transparency with low temperature processing of ZnO make it potential candidate to be employed for flexible transparent applications.[1,2] To utilize the ZnO based TFTs in flexible electronics, it is quite essential to obtain a good mechanical flexibility of each layer with no crack and excellent adhesion between the layers to

avoid delamination as the substrates are frequently subjected to large tensile or compressive strain, which can substantially degrade the device performance. However, in ZnO based TFTs, semiconducting layer (ZnO), electrode material (ITO) and dielectric layer (SiO_2), all are intrinsically brittle, and they could be easily cracked and delaminated during bending conditions. Therefore, it is important to understand the characteristics of the mechanical reliability of the ZnO TFTs device for the implementation of flexible electronics. Several research groups have investigated ZnO TFTs.[3,4] However, they focused on the development of new materials and fabrication methods as well as characterization of the electrical and optical performances. Stretchable ZnO TFTs were fabricated on the flexible substrate using transfer printing process with strain-induced wavy geometry,[5] which were developed in the Rogers Group.[6,7] Few studies investigated ZnO TFTs and circuit bent to a specific radius.[8,9] However, research regarding the mechanical reliability of ZnO TFTs is still limited, leading to a lack of available practical data.[9]

In this study, we fabricated flexible transparent ZnO TFTs with transfer printing process. The flexibility and mechanical reliability of ZnO TFTs were investigated by bending tests. Stress analysis during bending was also performed by the finite element method (FEM).

2. Experimental Method

Figure 1 presents a schematic cross-sectional view of a ZnO TFT. To fabricate the transparent thin film transistor, ZnO, SiO_2 and ITO were used as the active layer, insulator and electrode, respectively. A 300 nm thick germanium (Ge) sacrificial layer and a SiO_2 buffer layer were deposited onto the silicon mother substrate by *e*-beam evaporation. For oxidation of as-deposited Ge film, SiO_2/Ge/Si substrate was annealed at 450°C because it can be dissolved in water as an oxide.[10,11] After thermal oxidation of Ge, a 100 nm ITO film, as gate electrode was deposited on the SiO_2 buffer layer by RF magnetron sputtering. A 100 nm SiO_2 insulator layer was then deposited using plasma-enhanced chemical vapor deposition (PECVD) equipment. A 100 nm undoped ZnO film with 99.99% purity was sputtered using a RF magnetron sputtering system at room temperature. After deposition of the ZnO film, the devices were annealed at 350°C to enhance the electrical properties, and then ITO layer was deposited as the source/drain electrodes. To protect the device, an encapsulation film (SU-8) was coated with the thickness of 1 μm onto the top of the device using a spin coater. Next, we etched the SiO_2 using reactive ion etching through a patterned layer of photoresist to isolate the active device islands connected mechanically by thin bridges of SU-8/SiO_2.

Figure 2(a) shows a schematic diagram of the steps for fabricating a flexible ZnO TFT array using transfer printing method. The thin ZnO TFT array can be lifted from the Si wafer using a polydimethylsiloxane (PDMS) elastomeric stamp after removing the underlying Ge sacrificial layer with water. The released thin ZnO TFT array on PDMS can be transfer-printed again on to a PET substrate
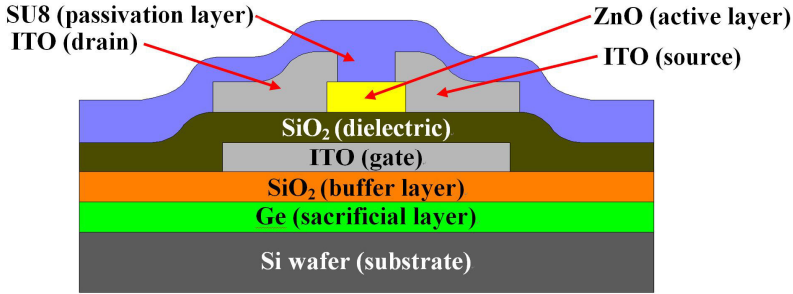
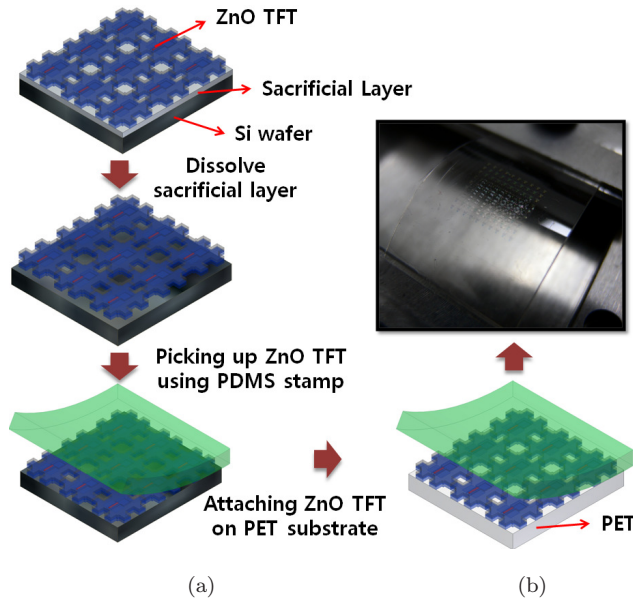Fig. 1. Schematic diagram of ZnO TFT fabricated on Si wafer.

Fig. 2. (a) Schematics of transfer printing method of ZnO TFT array from Si wafer to PET substrate using PDMS stamp. (b) Optical image of ZnO TFTs array on PET substrate.

with a thickness of 188 μm, which was coated with NOA UV curable adhesive to improve bonding between the ZnO TFT array and PET substrate. A detailed transfer printing process has been described elsewhere.[6,7] Figure 2(b) presents the optical image of the fabricated ZnO TFT array on PET sheet. The size of ZnO TFT array was 7.25 mm $\times$ 6.95 mm and ZnO TFT array was composed of ninety ZnO TFTs. The total thickness of ZnO TFT was around 750 nm. The resulting arrays of ZnO TFT were mechanically flexible due to the bending ability of the PET sheet and the small device thickness (<1 μm).

Good mechanical flexibility or reliability is essential for realizing the practical applications to flexible electronics. The flexibility of ZnO TFTs on PET substrate
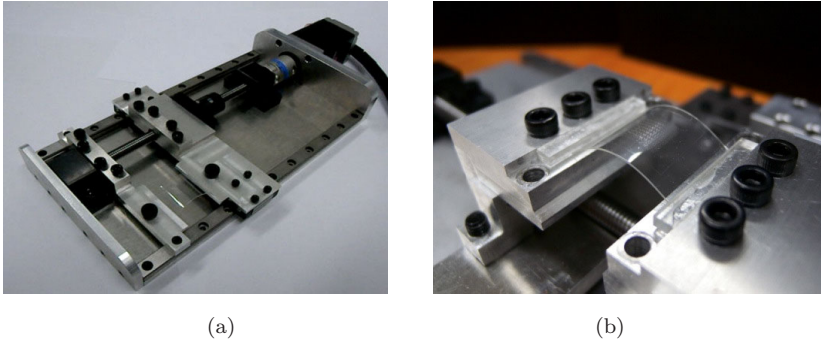
(a)   (b)

Fig. 3. Photographs of (a) bending test machine and (b) ZnO TFTs array under bending test on PET substrate.

was investigated using a computer-controlled bending test machine as shown in Fig. 3. Four-point probe station, with an optical microscope was used to observe the existence of cracks on the device. Dynamic fatigue bending tests were carried out using a cyclic bending test machine over 2000 cycles at a frequency of 0.5 Hz. The bending radius (R) is calculated using Eq. (1)[12]

$$\text{Bending radius } (R) = \frac{L}{2\pi\sqrt{\dfrac{dL}{L} - \dfrac{\pi^2 h_s^2}{12L^2}}} \tag{1}$$

where L, dL/L and h_s denote the initial length, the applied strain and substrate thickness, respectively.

Normal bending strain can be calculated using the following Eq. (2)[12]

$$\text{Strain} = \frac{h_s}{2R}. \tag{2}$$

During the mechanical reliability test, the transfer characteristics and I–V curves of the ZnO TFTs were measured using an Agilent HP 4155C semiconductor parameter analyzer.

3. Results and Discussion

Figure 4 shows the transmittance of the ZnO device including PET substrate, which is approximately 78% for wavelengths between 400 and 1000 nm. Figure 5 shows the typical transfer characteristics curve and I–V curves of the ZnO TFTs, which is measured within the range of gate voltages (V_{GS}) from -20 to 30 V at a fixed drain voltage (V_{DS}) of 5 V. The ZnO TFTs before transfer showed an on–off ratio of approximately $\sim 10^5$, an electron mobility of ~ 0.49 cm^2/Vs and a threshold voltage (V_{th}) of ~ 12 V. Linear and saturation region are shown in Fig. 5(b) clearly. According to Fig. 5(b) and using the equation $V_{\text{DS}} = V_{\text{GS}} - V_{\text{th}}$, V_{th} is calculated and found to be in the range of $5 \sim 8$ V. It indicates that with the increase of applied V_{GS}, the value of drain current increases in the saturation region due to the
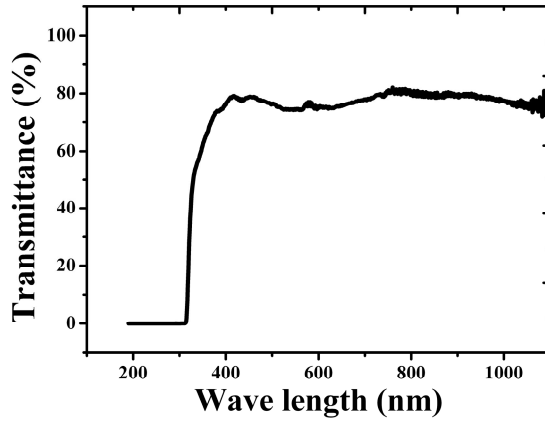
Fig. 4.   Optical transmittance of ZnO TFTs device including PET substrate.
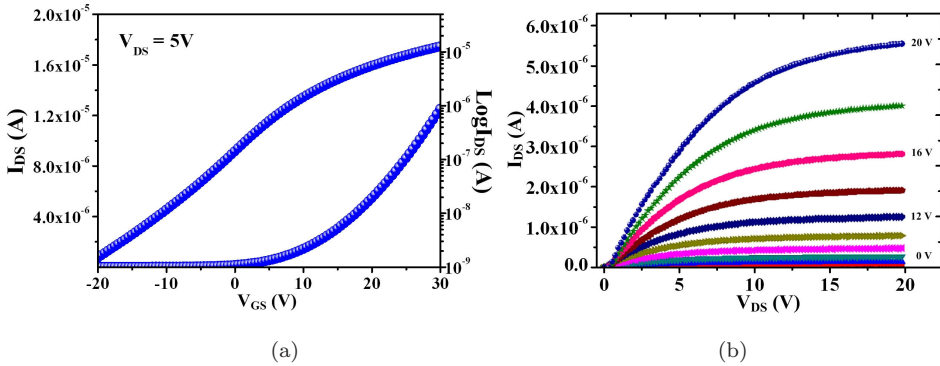

Fig. 5.   Electrical characteristics of transfer printed ZnO TFT (a) transfer curve, (b) *I*–*V* curve.

DIBL (drain induced barrier lowering). The drain current (I_{DS}) can be represented by the following equation

$$I_{\mathrm{DS}} = \frac{1}{2}(\mu_n C_{\mathrm{ox}})\frac{W}{L}(V_{\mathrm{GS}} - V_{\mathrm{th}})^2 \tag{3}$$

where W and L are the width and length of channel layer, respectively, C_{ox} is the capacitance per unit area of the gate insulating layer, and V_{GS} and V_{DS} are the gate-source and drain-source voltage, respectively. The value of mobility can be calculated from Eq. (3) using the transfer characteristics shown in Fig. 5(a).

Flexibility of the ZnO TFTs was tested with decreasing the bending radius. To measure the TFT performance at a specific bending radius, the bending machine was paused, and the transfer characteristic was measured immediately for each new bending radius. Two or three TFTs on the top of the bent surface was measured since they are subject to the maximum tensile stress when they were bent. The typical transfer curves and calculated mobility of ZnO TFTs, at bending radius
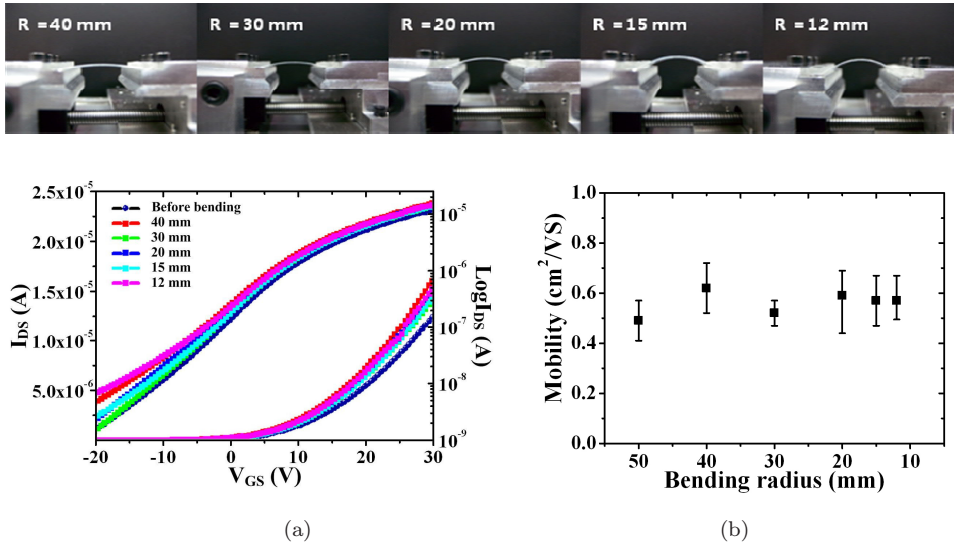
Fig. 6. (a) Transfer curves of bent ZnO TFT at bending radius of 40 mm to 12 mm, (b) mobility of bent ZnO TFT at bending radius of 40 mm to 12 mm.
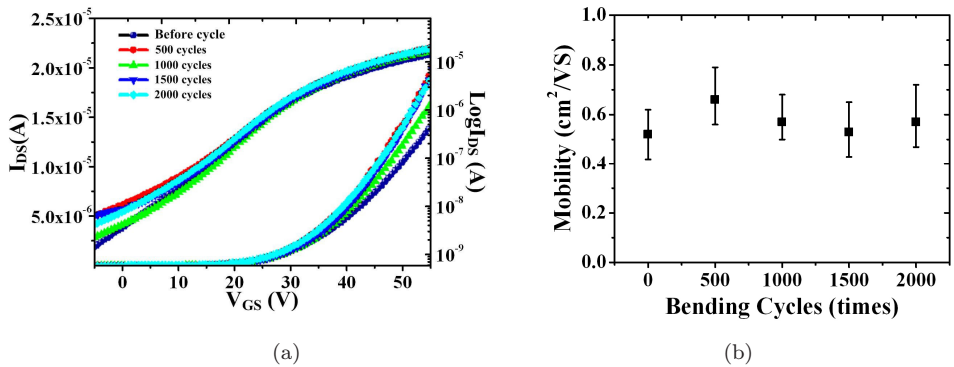

Fig. 7. (a) Transfer curves and (b) variation of mobility of ZnO TFT for bending fatigue test at bending radius of 40 mm.

of 40 mm to 12 mm are shown in Fig. 6. For bending radii up to 12 mm that corresponds to a strain value of 0.78%, we have observed only small change in transfer curves and device mobility. In addition, any cracks or damages of the ZnO TFTs were not observed. These results suggest that the ZnO TFTs may have good flexibility, even at the bending radius of 12 mm.

The dynamic bending fatigue tests were carried out at a frequency of 0.5 Hz over duration of 2000 cycles. The bending radius was fixed at 20 mm which correspond to a strain value of 0.47%. Figures 7(a) and 7(b) show the transfer curves and the variation of device mobility as a function of bending cycles. During the 2000 cycles of the bending fatigue tests, ZnO TFTs showed the excellent mechanical reliability.
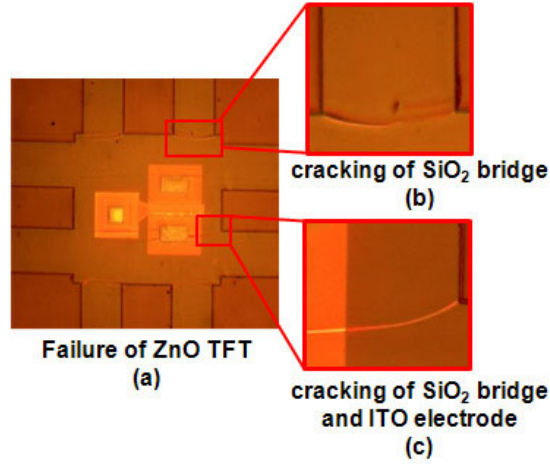
Fig. 8. Optical image of cracks generated ZnO TFT and magnified view of cracking of SiO_2 bridge and ITO electrode at the bending radius of 11 mm, which corresponds to normal strain 0.86%. (a) Failed ZnO TFT, (b) crack of SiO_2 bridge area, (c) crack of SiO_2 bridge and ITO electrode.

Table 1. Material properties of the ZnO TFT used in numerical study.

Material	Young's modulus (GPa)	Poisson's ratio
ITO (source/drain/gate)	116	0.35
SiO_2 (buffer layer, dielectric layer)	70	0.17
ZnO (active layer)	135	0.36
SU-8 (passivation layer)	3.4	0.4
PET (substrate)	5.5	0.4

When ZnO TFT array was bent to bending radius of 11 mm, the cracks mainly occurred at the SiO_2 bridge due to the stress concentration as shown in Fig. 8(b). It was thought that the initial cracking of destructed SiO_2 bridge leads to secondary crack of the ITO electric pad as shown in Fig. 8(c).

The strain, stress level of the ZnO TFT device during bending operation was estimated using the FEM. The stress level of the each layer of the ZnO TFT array was also calculated. The simulations were performed using the nonlinear finite element analysis package ANSYS, a commercial software. The mechanical properties for each layer are given in Table 1.[13−16]

Figure 9 shows the stress and strain level of each layer of ZnO TFT, which include ZnO active layer, ITO electrodes and SiO_2 buffer (or bridge) layer, at the bending radius of 11 mm. The strain value of ZnO, source-drain ITO electrode, gate ITO electrode and SiO_2 buffer layer was estimated to be 0.5%, 0.515%, 0.53% and 0.55%, respectively. Sharpe[13] reported that the tensile fracture strain of SiO_2 layer is 0.55%, and Chen *et al.*[14] showed that the tensile fracture strain of ITO electrode is around 1%. The simulation results indicate that the strain of SiO_2 layer is 0.55%,
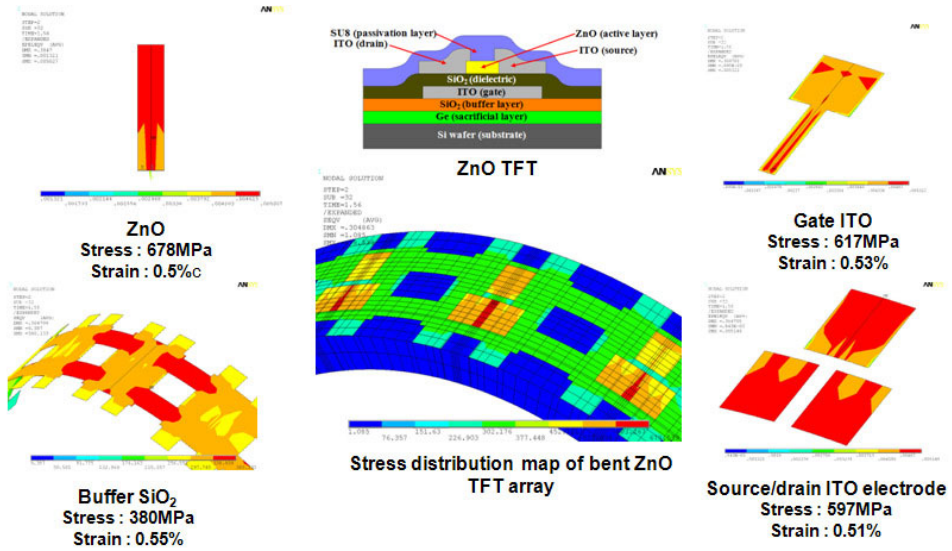
Fig. 9. Stress distribution map of the bent ZnO TFT and each layer of ZnO TFT including ZnO, ITO electrode, gate ITO electrode, and SiO_2 buffer layer.
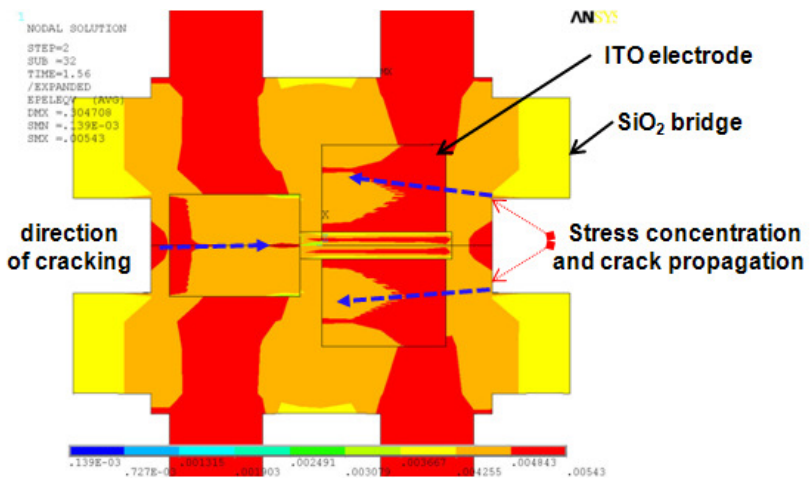

Fig. 10. Numerical simulation of stress concentrations and crack propagation of the SiO_2 layer and ITO electrode.

and reaches near the fracture stress level. Figure 10 shows the stress concentration of ITO and SiO_2 layer. The stress concentration was observed at the edge of the SiO_2 bridge layer. The numerical results were well matched with mechanical bending test results at which the most of cracks start to occur in connected parts between island and bridge due to the stress concentration. Therefore, it is inferred that the cracks
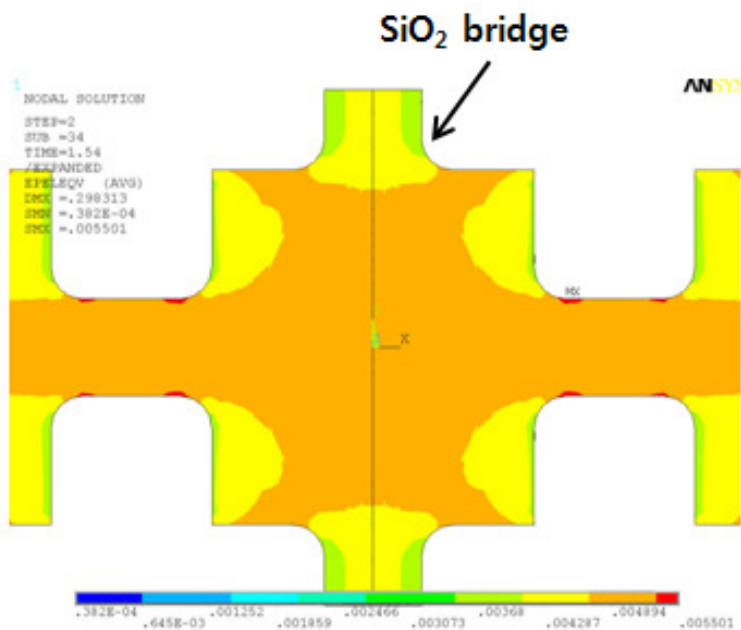
Fig. 11. Numerical simulation results using round SiO_2 bridge interconnect, the stress distribution map shows the dramatic stress reduction in ZnO TFT array

were initiated at the SiO_2 bridge layer and then propagated to ITO electrode. Since the SiO_2 film and ITO film are very brittle, they are prone to fracture. In order to improve the flexibility of device, the design of the connected parts is changed into a round shape. Numerical simulation results shown in Fig. 11 indicate the dramatic reduction of the stress for round shape SiO_2 bridge.

4. Conclusion

In this study, flexible and transparent ZnO TFTs on PET substrate were fabricated using transfer printing method. After device fabrication, the flexibility and mechanical reliability of ZnO TFTs were investigated by bending tests. Transfer curves and device mobility as a function of bending radius of ZnO TFT remain unchanged up to bending radius of 12 mm. During the 2000 cycles of the bending fatigue test at the bending radius of 20 mm, the ZnO TFT showed excellent mechanical reliability. For ZnO TFT array to bending radius of 11 mm, the cracks occurred at the connected parts between island and brittle SiO_2 bridge which start to initiate at the SiO_2 bridge layer and then propagated to ITO layer. The numerical simulation indicates that stress of SiO_2 layer reaches near the fracture stress level. The stress concentration was observed at the edge of the SiO_2 bridge layer. The further improvement in the flexibility of the device can be realized by using the round shape design of interconnecting bridges.

Acknowledgment

References

1. E. Fortunato, P. Barquinha, A. Pimentel, A. Goncalves, A. Marques, R. Martins and L. Pereira, *Appl. Phys. Lett.* **85** (2004) 2541.
2. P. F. Carcia, R. S. McLean, M. H. Reilly and G. Nunes, *Appl. Phys. Lett.* **82** (2003) 1117.
3. J. H. Chung, J. Y. Lee, H. S. Kim, N. W. Jang and J. H. Kim, *Thin Solid Films* **516** (2008) 5597.
4. C. S. Li, Y. N. Li, Y. L. Wu, B. S. Ong and R. O. Loutfy, *J. Phys. D: Appl. Phys.* **41** (2008) 125102.
5. K. Park, D. K. Lee, B. S. Kim, H. Jeon and N. E. Lee, *Adv. Funct. Mater.* **20** (2010) 3577.
6. D.-H. Kim, J.-H. Ahn, W. M. Choi, H.-S. Kim, T.-H. Kim, J. Song, Y. Y. Huang, Z. Liu, C. Lu and J. A. Rogers, *Science* **320 (**2008) 507.
7. J.-H. Ahn, H.-S. Kim, K. Lee, S. Jeon, S. Kang, Y. Sun, R. Nuzzo and J. Rogers, *Science* **314** (2006) 1754.
8. M. S. Oh, W. Choi, K. Lee, D. K. Hwang and S. Im, *Appl. Phys. Lett.* **93** (2008) 033510.
9. K. H. Cherenack, N. S. Münzenrieder and G. Tröster, *IEEE Electron Device Lett.* **31** (2010) 1254.
10. R. H. Kingston, *J. Appl. Phys.* **27** (1956) 101.
11. C. P. Liu, *Thin Solid Films* **415** (2002) 296.
12. S.-I. Park, J.-H. Ahn, X. Feng, S. Wang, Y. Huang and J. A. Rogers, *Adv. Funct. Mater.* **18** (2008) 2673.
13. W. N. Sharpe, J. Pulskamp, D. S. Gianola, C. Eberl, R. G. Polcawich and R. J. Thompson, *Mechanics* **47** (2007) 649.
14. Z. Chen, B. Cotterell and W. Wang, *Eng. Fract. Mech.* **69** (2002) 597–603.
15. I. Ozen, M. A. Gulgun and M. Ozcan, *Key Eng. Mater.* **264** (2004) 1225.
16. C. W. Ong, D. G. Zong, M. Aravind, C. L. Choy and D. R. Lu, *J. Mater. Res.* **18** (2003) 2464.